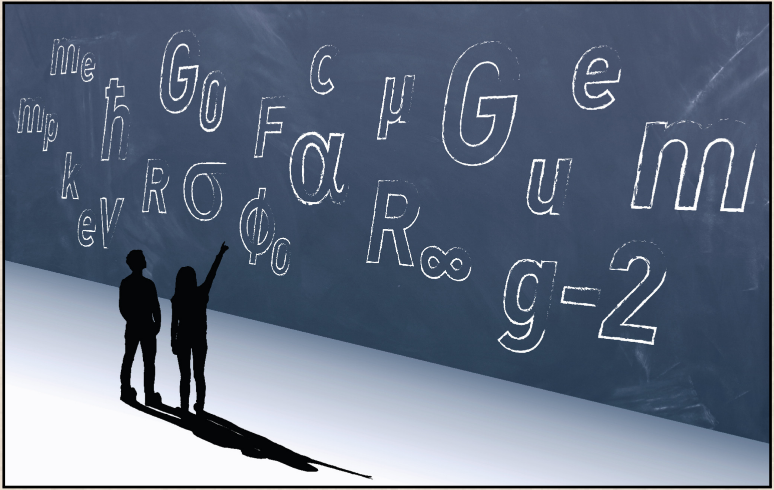

Status and prospects of the muon magnetic anomaly measurement at FNAL

Alberto Lusiani, for the FNAL Muon g-2 collaboration
Scuola Normale Superiore and INFN, sezione di Pisa

SCUOLA NORMALE SUPERIORE

INFN PISA

International Conference on Precision Physics and Fundamental Physical Constants (FFK2023), Vienna, Austria, 22-26 May 2023

Muon magnetic anomaly

particle x such as a muon, electron, proton, neutron

- magnetic moment $\vec{\mu}_x = g_x \frac{e}{2m_x} \vec{S}_x$,
  - e = absolute value of electron charge (used also for neutron)
  - $\vec{S}_x$ = spin (particle intrinsic angular momentum)
  - g_x = gyromagnetic ratio (defined also for neutral particles)
- classical charge distribution: $\rho_q/\rho_m = \text{constant} \quad \Rightarrow \quad g = 1$

leptons (electron, muon, tau): spin 1/2 fundamental point-like particles

- Standard Model
  - leading order: $g_e,\ g_\mu,\ g_\tau = 2$ (like Dirac eq.)
  - next to leading order: $g_e,\ g_\mu,\ g_\tau > 2$
- $a_x = \frac{g_x - 2}{2}$ anomalous gyromagnetic ratio or magnetic anomaly

- lepton g_x, a_x may be considered first most fundamental prediction of Standard Model

Muon $g-2$ anomaly motivated FNAL Muon $g-2$ experiment (E989)

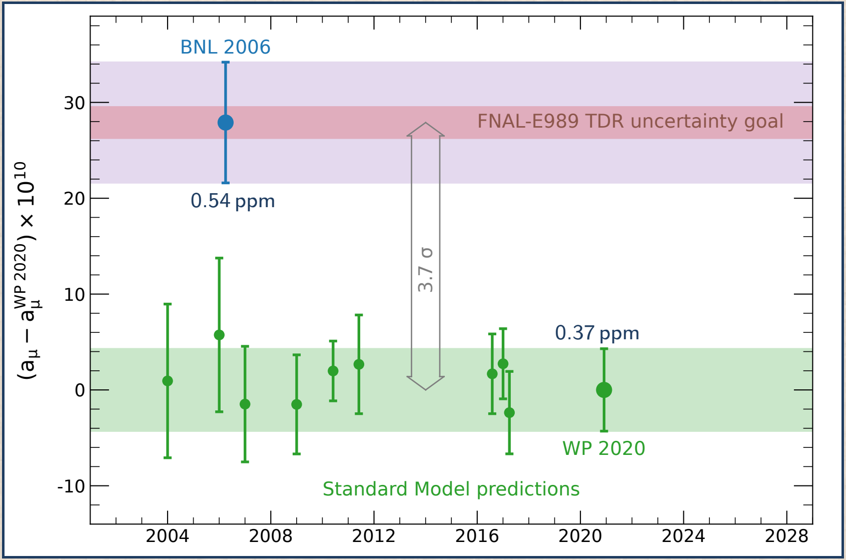

- BNL 2006: BNL-E821 Muon $g-2$ collaboration final report, Phys. Rev. D 73, 072003
- WP 2020: Muon $g-2$ theory initiative White Paper, Phys. Rept. 887 (2020) 1

FNAL-E989 vs. BNL-E821

FNAL-E989 design precision, compared to BNL-E821 final report (2006)

	BNL E821 (2006)	FNAL E989 final goal	
ω_a statistical	460 ppb	100 ppb	$\times$21 detected muon decays ($1.6 \cdot 10^{11}$)
ω_a systematic	210 ppb	70 ppb	faster calorimeter with laser calibration, tracker
ω_p systematic	170 ppb	70 ppb	more uniform B, improve NMR measurement
external measurements	negligible	negligible	
total	540 ppb	140 ppb	

ω_a: measured muon spin precession frequency in magnetic field
ω_p: measured proton spin precession frequency to measure magnetic field

FNAL-E989 Muon $g-2$ collaboration measurement in April 2021

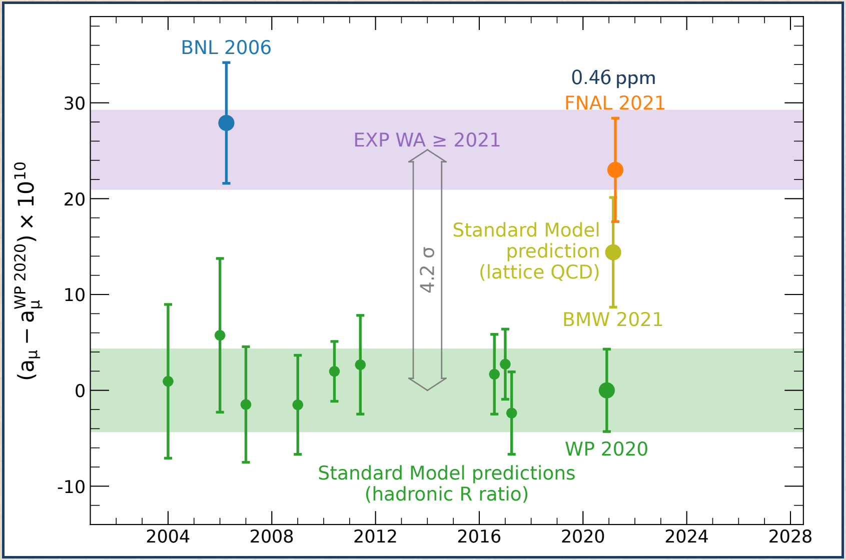

- FNAL-989 collaboration Run 1 measurement, Phys. Rev. Lett. 126, 141801
- BMW 2021, calculation with lattice QCD of HVP contribution, Nature volume 593, pages51-55 (2021)

Reached 21× BNL goal on 27 Feb 2023

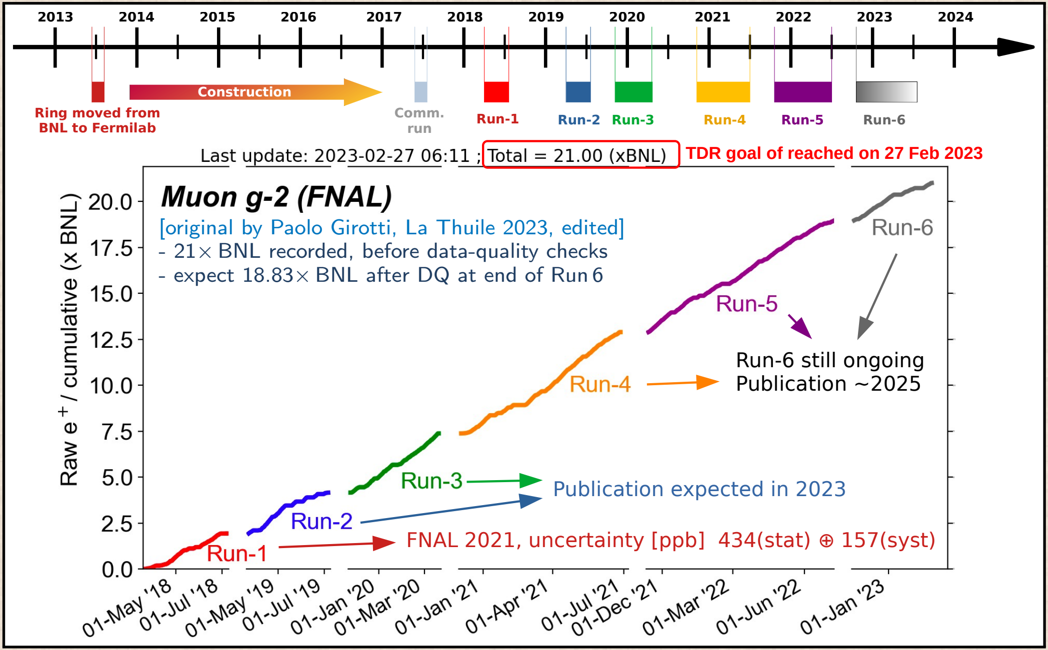

Motion and spin precession of muon in uniform magnetic field

muon spin precession relative to momentum

$$\omega_s - \omega_c = \omega_a$$

$$\boxed{-g_\mu \frac{eB}{2m_\mu} - (1-\gamma)\frac{eB}{m_\mu \gamma}} - \boxed{-\frac{eB}{m_\mu \gamma}} = \boxed{-a_\mu \frac{eB}{m_\mu}}$$

Larmor + Thomas precessions — cyclotron frequency — no γ!

- frequency measurements best for precision
- magnetic field NMR measurement also frequency
- angle between momentum and spin: $\varphi(t) = \omega_a t$

polarized muons in magnetic storage ring

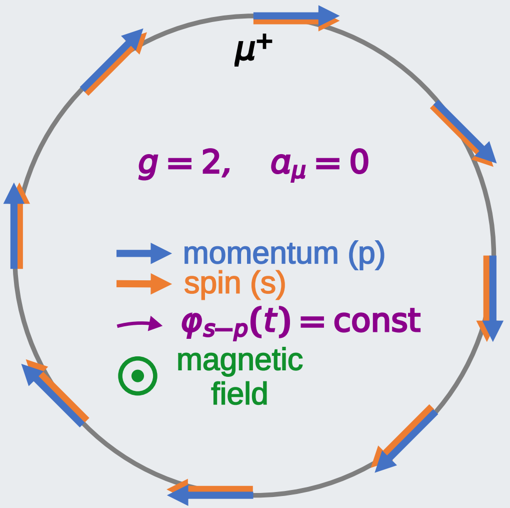

Motion and spin precession of muon in uniform magnetic field

muon spin precession relative to momentum

$$\omega_s \quad - \quad \omega_c \quad = \quad \omega_a$$

$$\boxed{-g_\mu \frac{eB}{2m_\mu} - (1-\gamma)\frac{eB}{m_\mu\gamma}} - \boxed{-\frac{eB}{m_\mu\gamma}} = \boxed{-a_\mu \frac{eB}{m_\mu}}$$

Larmor + Thomas precessions — cyclotron frequency — no γ!

- frequency measurements best for precision
- magnetic field NMR measurement also frequency
- angle between momentum and spin: $\varphi(t) = \omega_a t$

polarized muons in magnetic storage ring

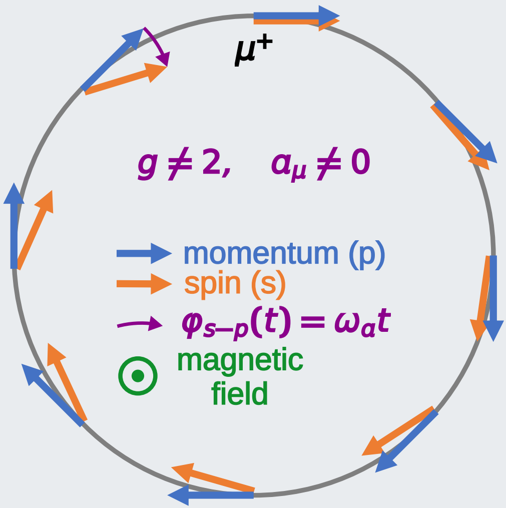

Beam focusing in storage ring, magic energy

- beam focusing
  - weak horizontal focusing provided by uniform magnetic field
  - vertical focusing with electric field quadrupoles
    - magnetic focusing prevails on quadrupole horizontal defocusing
- $$\vec{\omega}_a = -\frac{e}{m_\mu}\left[\quad a_\mu \vec{B} \quad - \quad \underbrace{\left(a_\mu - \frac{1}{\gamma^2 - 1}\right)(\vec{\beta}\times\vec{E})}_{E \text{ field correction}} \quad - \quad \underbrace{a_\mu \frac{\gamma}{\gamma+1}\left(\vec{\beta}\cdot\vec{B}\right)\vec{\beta}}_{\text{pitch correction}} \quad \right]$$
- magic energy, corresponding to $p_\mu^{\text{magic}} = 3.094\,\text{GeV}$ and $\gamma = 29.3$, zeroes E field correction

Production of polarized muons

- dump 8 GeV protons on target to produce pions
- select pions with momemtum $p \simeq 3.11$ GeV
- let them decay into muons
- in pion rest frame, parity violation in pion decay causes μ^+ spin aligned opposite to momentum vector
- in laboratory frame, highest energy muons are >90% polarized

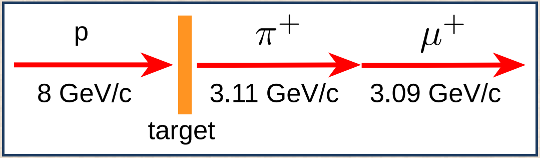

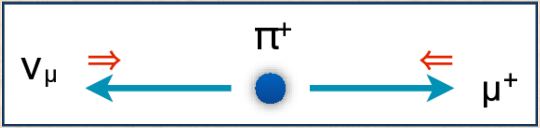

- with 8 GeV protons on target, μ^+ are produced $\sim 4\times$ more frequently than μ^-

Rate of high-energy muon-decay electrons modulated with $\cos \omega_a t$

- because of parity violation in muon decay, decay electrons peak along muon spin

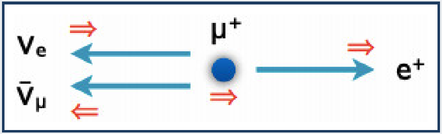

- electrons decaying along muon momentum have highest energy in laboratory frame
- $N_e(E_e > E_t) = N_{e0} e^{-t/\tau_\mu}(1 + A \cos \omega_a t)$

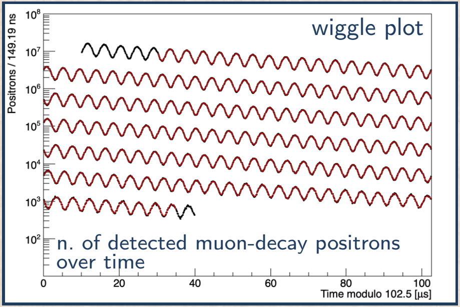

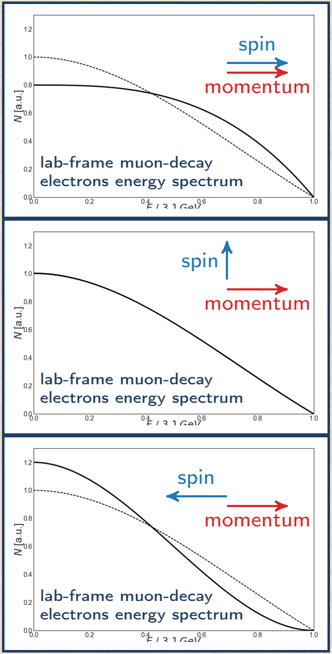

Muon production, storage and decay at FNAL

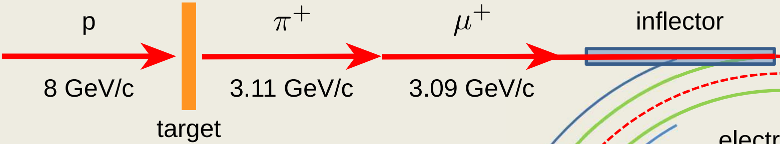

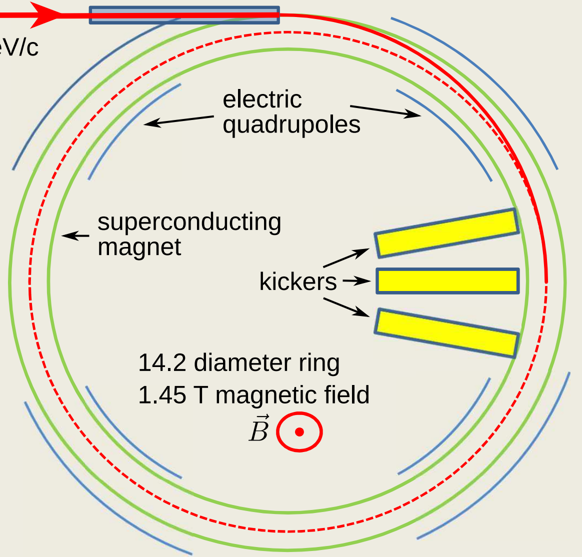

- FNAL booster+recycler: 12 Hz rate of 120 ns-long 10^{12} 8 GeV proton bunches
- pions focused with lithium lens
- pions with $p = 3.11$ GeV $\pm$ 10% selected
- 3.09 GeV 95% polarized muons accepted in delivery ring, separation from p's and π's
- inflector magnet cancels storage ring field
- kickers pulsed B field puts muons in orbit
- $\sim$5000 stored muons per fill, 12 Hz fills
- $\sim$500 high-energy electrons detected per fill
- more muons than at BNL
- less p, π contamination than at BNL

Magnetic kickers put muons into correct orbit

- 3 pulsed electro-magnets
- 3 – 4 kA peak current
- ~130 ns pulse duration, shorter than cyclotron period (149.2 ns)

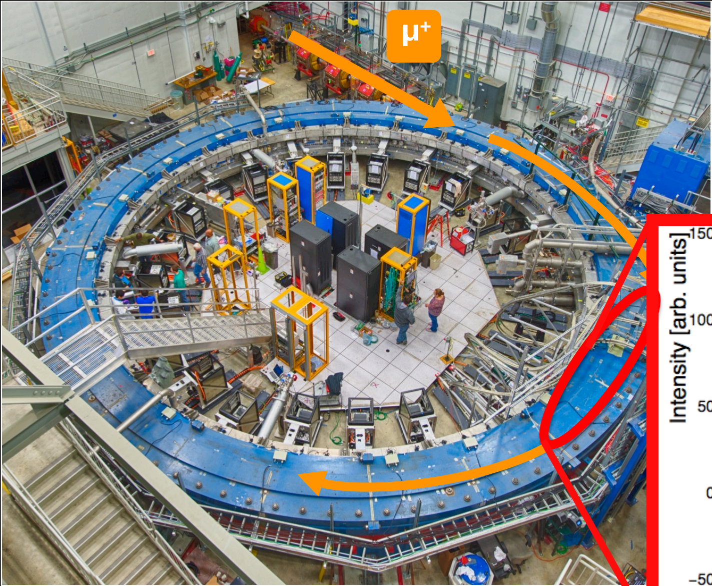

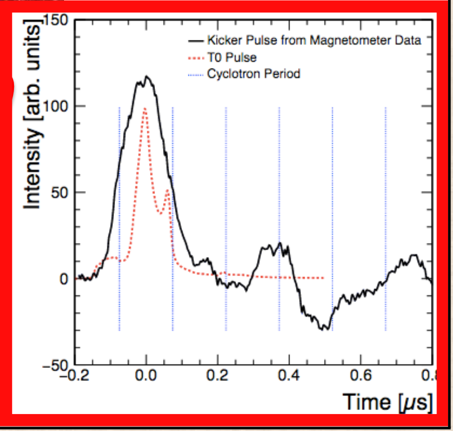

Electric quadrupoles focus beam vertically

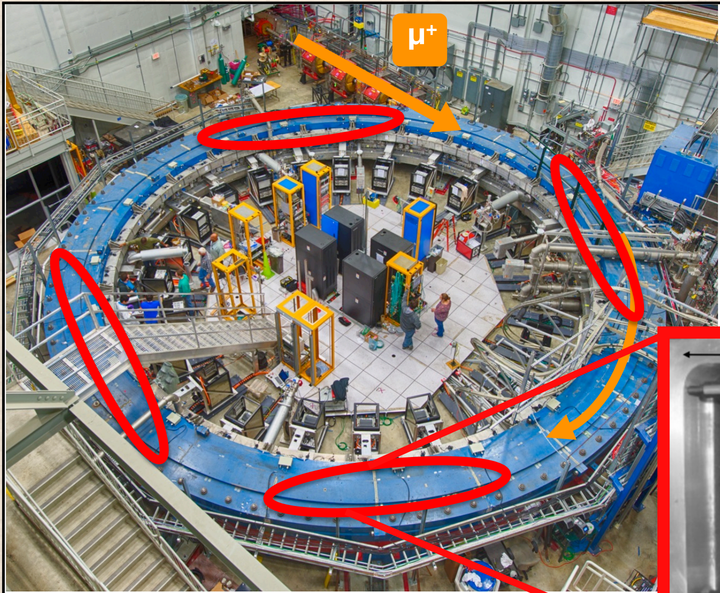

- operated in 15 – 21 kV range
- pulsed to avoid spatial charge accumulation
- bend beam before measurement to remove beam outer tails with beam collimators

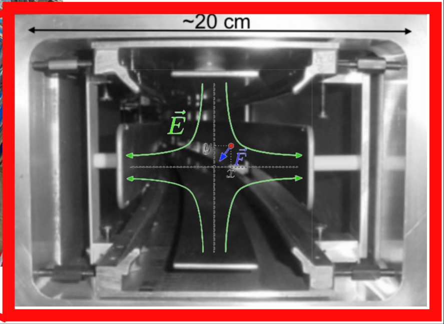

Two tracker modules

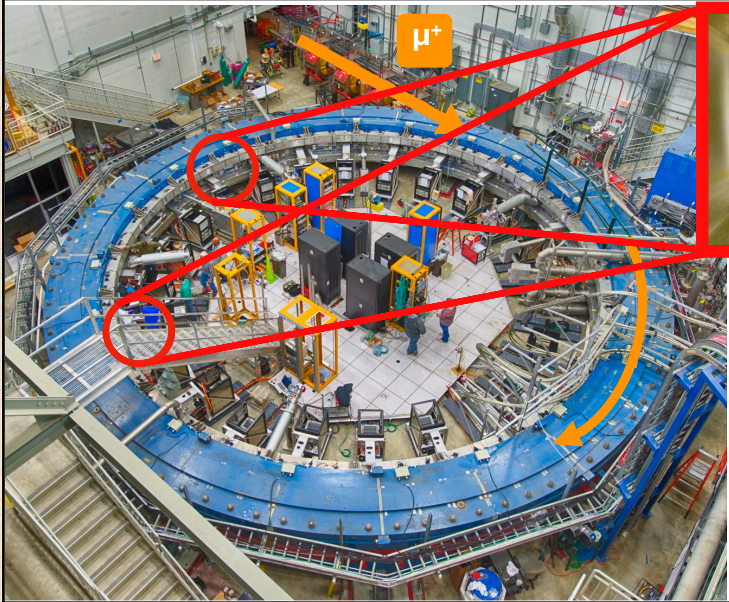

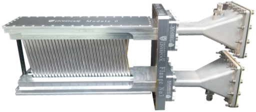

each tracker

- 8 modules
- 128 straw chambers each
- trace back muon decay points

24 calorimeter modules

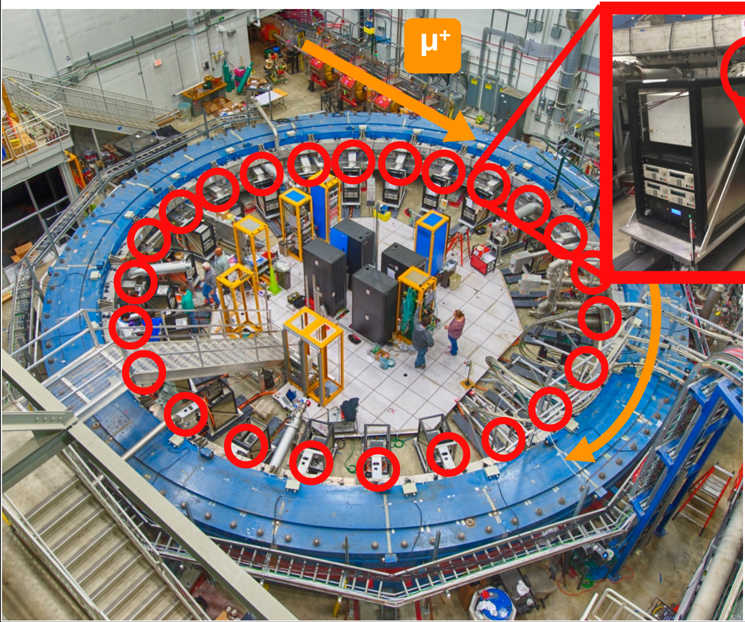

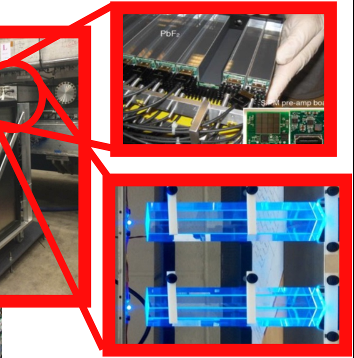

each module

- 6×9 PbF_2 crystals array
- 2.5 cm×2.5 cm×14 cm, 15 X_0
- readout Cherenkov light at 800 MHz with SiPMs
- continuos gain monitoring with laser system pulses

Conceptual formula for $R'_\mu(T) = \omega_a/\tilde{\omega}'_p(T)$

$$R'_\mu(T) = \frac{\omega_a}{\tilde{\omega}'_p(T)} \overset{\text{conceptually}}{=} \frac{\omega_a^{\mathrm{m}} \left(1 + C_e + C_p + C_{\mathrm{ml}} + C_{\mathrm{pa}} + C_{\mathrm{dd}}\right)}{\langle \omega'_p(T)(x,y,\varphi) \times M(x,y,\varphi)\rangle \left(1 + B_k + B_q\right)}$$

ω_a^{m} - muon-spin precession

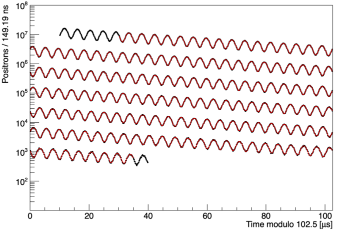

$\omega'_p(T)(x,y,\varphi)$ - B field

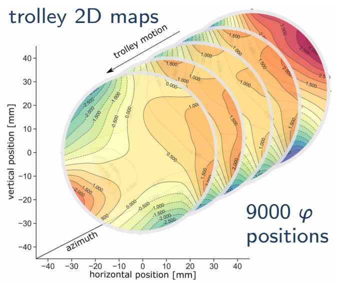

$M(x,y,\varphi)$ - μ^+ distribution

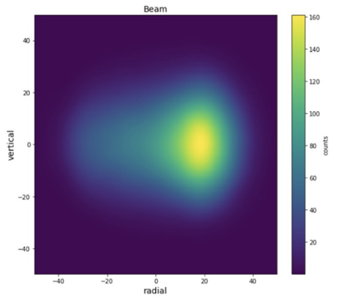

- ω_a: muon spin precession frequency
- C_x: corrections to ω_a for E field, pitch, muon loss, phase accetpance, differential decay
- $\omega'_p(T)$ precession frequency of shielded proton spin in spherical water sample at $T = 34.7\,^\circ\mathrm{C}$
- B_x: corrections to ω_p for quadrupole and kickers transient fields

Muon precession frequency ω_a fit with threshold (T) method

fit model for number of detected positrons with $E > 1.7$ GeV in time bins from 30 to 650 μm

$$N_{e^+}(t) = N_0 \cdot N_x(t) \cdot N_y(t) \cdot \Lambda(t) \cdot e^{-t/\gamma\tau_\mu} \cdot [1 + A_0 \cdot A_x(t) \cdot \cos(\omega_a t + \phi_0 \cdot \phi_x(t))]$$

$$N_x(t) = 1 + e^{-t/\tau_{\mathbf{CBO}}} A_{N,x,1,1} \cos\left(\omega_{\text{CBO}} t + \phi_{N,x,1,1}\right) + e^{-2t/\tau_{\mathbf{CBO}}} A_{N,x,2,2} \cos\left(2\omega_{\text{CBO}} t + \phi_{N,x,2,2}\right)$$

$$N_y(t) = 1 + e^{-t/\tau_y} A_{N,y,1,1} \cos\left(\omega_y t + \phi_{N,y,1,1}\right) + e^{-2t/\tau_y} A_{N,y,2,2} \cos\left(\omega_{\text{VW}} t + \phi_{N,y,2,2}\right)$$

$$A_x(t) = 1 + e^{-t/\tau_{\mathbf{CBO}}} A_{A,x,1,1} \cos\left(\omega_{\text{CBO}} t + \phi_{A,x,1,1}\right)$$

$$\phi_x(t) = 1 + e^{-t/\tau_{\mathbf{CBO}}} A_{\phi,x,1,1} \cos\left(\omega_{\text{CBO}} t + \phi_{\phi,x,1,1}\right)$$

$$\Lambda(t) = 1 - K_{\text{loss}} \int_0^t e^{t'/\gamma\tau} L(t') dt'$$

$$\omega_{\text{CBO}} \cdot t \to \omega_{\text{CBO}} \cdot t + A_1 e^{-t/\tau_1} + A_2 e^{-t/\tau_2}$$

$$\omega_y(t) = \kappa_y \cdot \omega_{CBO}(t) \left(\frac{2\omega_c}{\kappa_y \cdot \omega_{CBO}(t)} - 1 \right)^{1/2}$$

$$\omega_{\text{VW}}(t) = \omega_c - 2\omega_y(t)$$

- from 16 to 27 (22 typical) fit parameters, depending on analysis group and measurement method
- actual measurement uses asymmetry-weighted (A) method, about 10% more precise

Fourier transform of fit residuals of ω_a fit

- beam frequencies appear (in red) for simple 5 parameter fit, $N(t) = N_0 e^{-t/\tau_\mu} [1 + A\cos(\omega_a t + \varphi)]$
- no beam frequencies peaks for full ∼22 parameter fits accounting for muon loss and beam dynamics

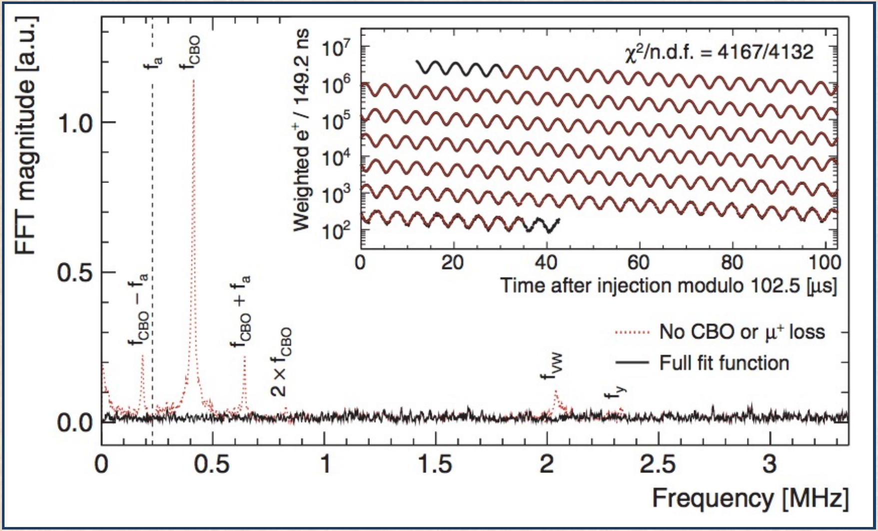

7 analysis groups, 19 blind ω_a measurements on each of 3 datasets

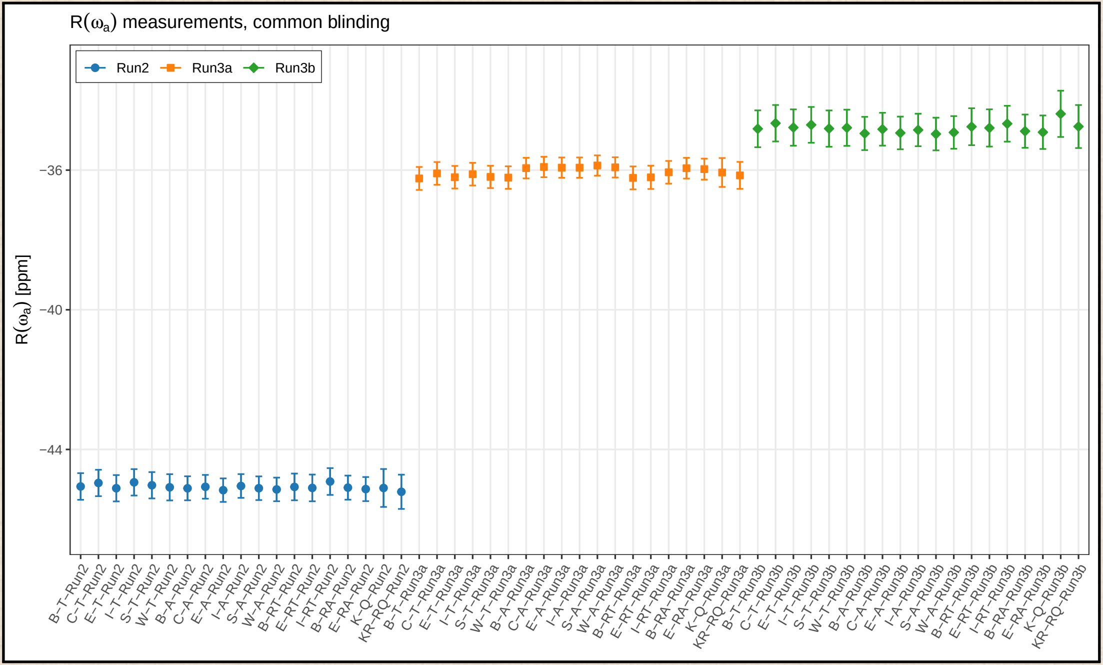

Storage ring magnet, magnetic field measurement

- superconductive magnet cooled at ~5 K
- 1.45 T vertical uniform magnetic field
- shimmed passively with iron foils
- actively stabilized with correction coils
- <50 ppm RMS B field homogeneity
- <14 ppm RMS B field azimuth-averaged

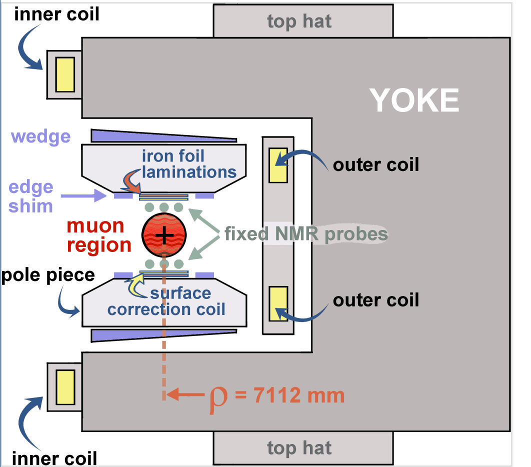

magnetic field measurement with NMR probes

- measured as proton spin precession frequency
- 378 fixed probes to track field continuously
- trolley with probes maps magnetic field periodically during off-beam intervals
- trolley probes calibrated with reference NMR probe

B_q, correction for transient B field produced by electric quadrupoles

- electric quadrupoles are pulsed (to prevent static charge accumulation)
- plates vibration perturbs magnetic field
- special NMR probes measure the transient field perturbation in muon region
- much better measured in Run 2+ vs. Run 1

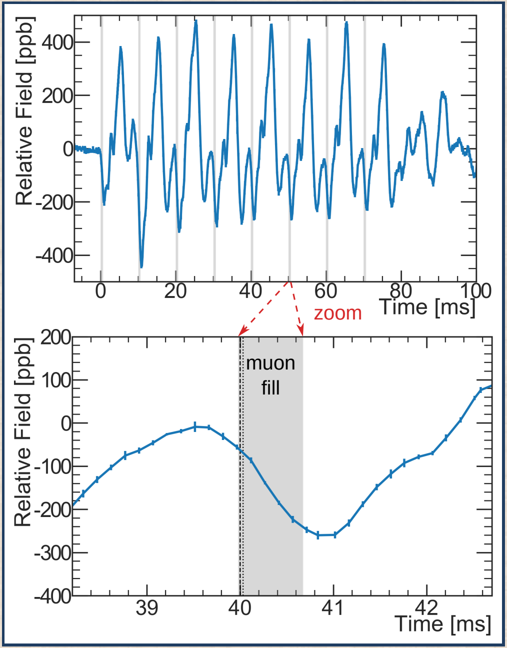

B_k, correction for transient B field produced by kicker magnets

- kicker magnets pulsed before start of fit window
- induced eddy currents perturb magnetic field inside fit window
- magnetic field perturbation measured with a Faraday effect magnetometer
- much better measured in Run 2+ vs. Run 1

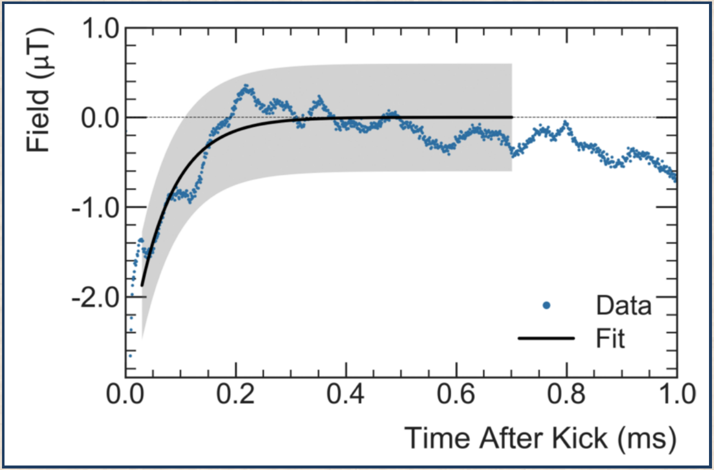

Improvements with respect to Run 1

- refinements in ω_a fits reduced systematics
- refinements in ω_p
- fixed broken resistors that affected quadrupole operations in Run 1
  - significantly recuced phase acceptance correction and its uncertainty
  - significantly reduced muon losses
- kickers power increased, towards end of Run 3 beam reached nominal position
  - in Run 1 and part of Run 2,3 larger E field correction
- active RF system reduces amplitude of horizontal beam oscillations (only since Run 5
- significantly better measurements of transient fields

Personal estimate of Run 2+3 ω_a uncertainties

	Run 1	Run 2+3	design	notes
ω_a^m (statistical)	434	200	100	
ω_a^m (systematic)	56	24		
C_{BD}	93	56		
- C_e	53	53		my guestimate
- C_p	13	10		
- C_{pa}	75	13		
- C_{ml}	5	3		
- C_{dd}	-	7		one small term still missing
ω_a total systematic	109	61	70	
$\omega'_p(T)$	56	46		
$\tilde{\omega}'_p(T)$ (transient fields)	99	19		
- B_q	92	14		
- B_k	37	13		
$\tilde{\omega}'_p(T)$ (total)	114	50	70	
R_μ (total systematic)	157	79	100	
total	462	215	140	

Expected precision on a_μ vs. number of BNL samples after quality cuts

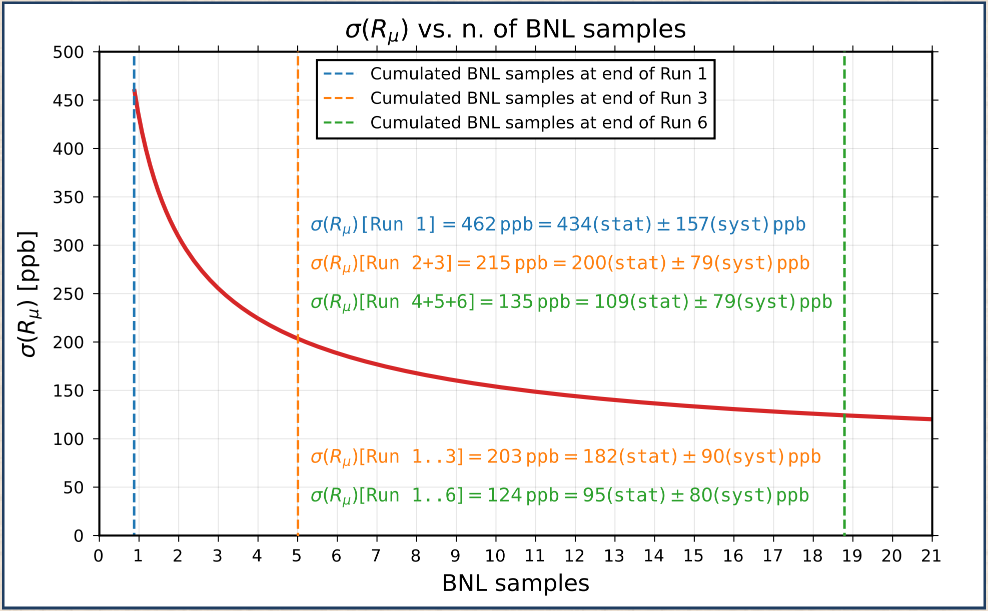

Calculation of the muon magnetic anomaly

$$a_\mu = \left[\frac{\omega_a}{\tilde{\omega}'_p(T)}\right] \cdot \left[\frac{\mu'_p(T)}{\mu_e(\mathrm{H})}\right] \left[\frac{\mu_e(H)}{\mu_e}\right] \left[\frac{m_\mu}{m_e}\right] \left[\frac{g_e}{2}\right]$$

(equivalent to $a_\mu = \dfrac{\omega_a/\omega_p}{\mu_\mu/\mu_p - \omega_a/\omega_p}$ using CODATA constants)

measurements by the Muon $g-2$ collaboration

- ω_a — precession of muon spin relative to momentum rotation in magnetic field
- $\tilde{\omega}'_p(T)$ — precession frequency of shielded proton spin in spherical water sample at $T = 34.7\,°\mathrm{C}$ in muon-beam-weighted magnetic field, $\tilde{\omega}'_p(T) = \langle \omega'_p(T)(x,y,\varphi) \times M(x,y,\varphi)\rangle$

notation

- $\mu'_p(T)$ — magnetic momentum of proton in spherical water sample at 34.7 °C
- $\mu_e(\mathrm{H})$ — magnetic momentum of electron in hydrogen atom

external measurements

- $\mu'_p(T)/\mu_e(H)$ — 10.5 ppb precision, Metrologia 13, 179 (1977)
- $\mu_e(H)/\mu_e$ — 5 ppq (negligible) theory QED calculation, Rev. Mod. Phys. 88 035009 (2016)
- m_μ/m_e — 22 ppb precision CODATA 2018 fit, primarily driven by LAMPF 1999 measurements of muonium hyperfine splitting, Phys. Rev. Lett. 82, 711 (1999)
- $g_e/2$ — 0.28 ppt (negligible), Phys. Rev. Lett. 100, 120801 (2008)

Expected precision of final FNAL Run 1..3 a_μ measurement in 2023

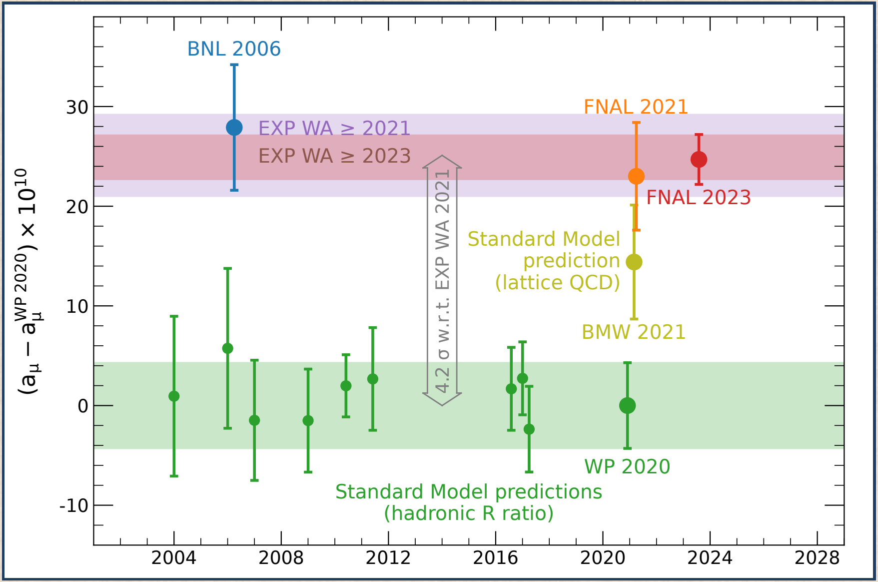

Expected precision of final FNAL Run 1..6 a_μ measurement in 2025

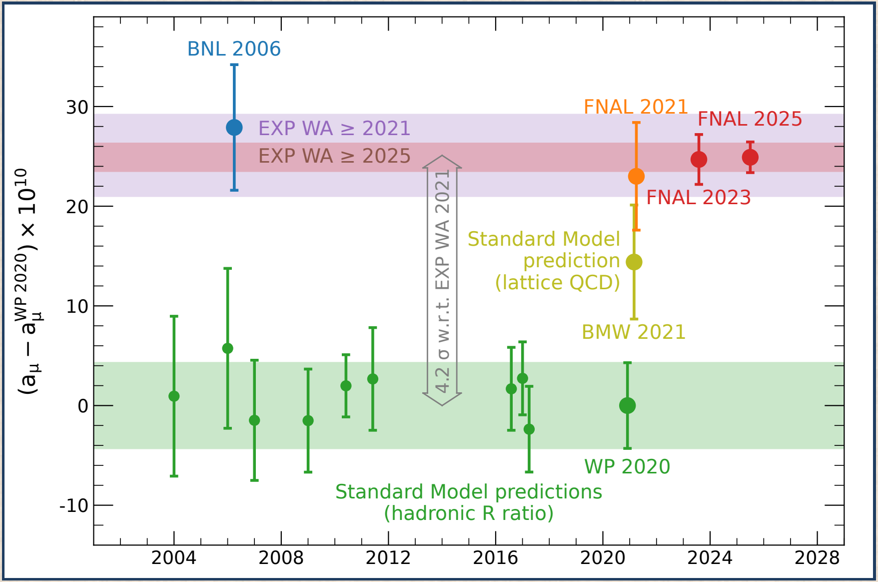

Thanks for your attention!

Backup slides

FNAL Muon $g-2$ collaboration

USA
- Boston
- Cornell
- Illinois
- James Madison
- Kentucky
- Massachusetts
- Michigan
- Michigan State
- Mississippi
- North Central
- Northern Illinois
- Regis
- Virginia
- Washington

USA National Labs
- Argonne
- Brookhaven
- Fermilab

China
- Shanghai Jiao Tong

Germany
- Dresden
- Mainz

Italy
- Frascati
- Molise
- Naples
- Pisa
- Roma Tor Vergata
- Trieste
- Udine

Korea
- CAPP/IBS
- KAIST

Russia
- Budker/Novosibirsk
- JINR Dubna

United Kingdom
- Lancaster/Cockcroft
- Liverpool
- Manchester
- University College London

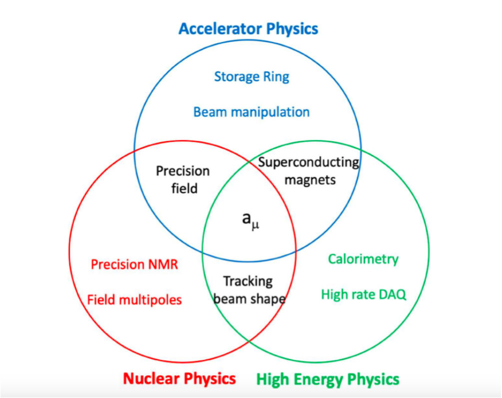

~200 collaborators
~40 institutions
7 countries

Focusing electric field and magic energy

in presence of (focusing) electric field and motion not perfectly transverse to magnetic field

$$\vec{\omega}_a = -\frac{e}{m_\mu}\left[a_\mu \vec{B} - \left(a_\mu - \frac{1}{\gamma^2-1}\right)(\vec{\beta}\times\vec{E}) - a_\mu \frac{\gamma}{\gamma+1}\left(\vec{\beta}\cdot\vec{B}\right)\vec{\beta}\right]$$

CERN 1975-, BNL, FNAL

$$p_\mu^{\text{magic}} = 3.094\ \text{GeV} \quad\Rightarrow\quad \gamma = 29.3$$

$$\Rightarrow \quad \left(a_\mu - \frac{1}{\gamma^2-1}\right) \simeq 0$$

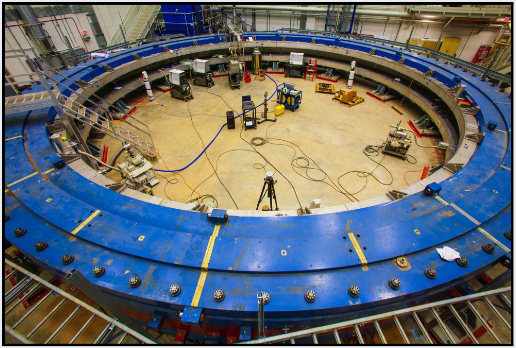

J-PARC E34

ultra-cold muons

$$E = 0 \quad\Rightarrow\quad \vec{\beta}\times\vec{E} = 0$$

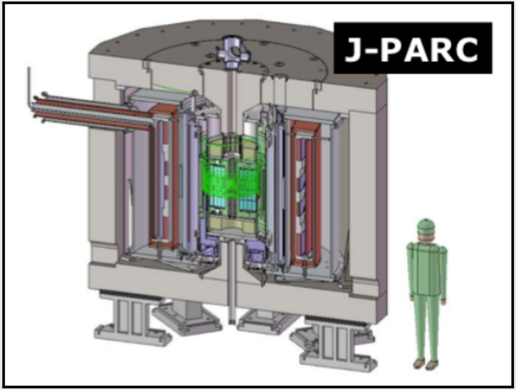

Beam dynamics frequencies

			f [MHz]	T [μs]
Anomalous precession	f_a		0.2291	4.3649
Cyclotron	f_c		6.7024	0.1492
Horizontal betatron	f_x	$= f_c\sqrt{1-n}$	6.2874	0.1590
Vertical betatron	f_y	$= f_c \cdot \sqrt{n}$	2.3218	0.4307
Coherent betatron oscillation	f_{CBO}	$= f_c - 1 \cdot fx$	0.4150	2.4097
Vertical oscillation	f_{VO}	$= f_c - 1 \cdot fy$	4.3806	0.2283
Vertical waist	f_{VW}	$= f_c - 2 \cdot fy$	2.0589	0.4857

field index $n = 0.12$

Extend ω_a fit model to account for lost muons on collimators

- some muons hit collimators and are lost
- muon loss rate during a fill measured with 3-4-5 coincidences of m.i.p. on calorimeters
- overall normalization of muon loss included as fit parameter

muon loss vs. time

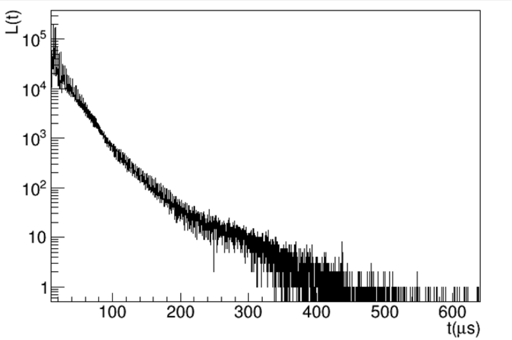

energy in calorimeter vs. momentum in tracker

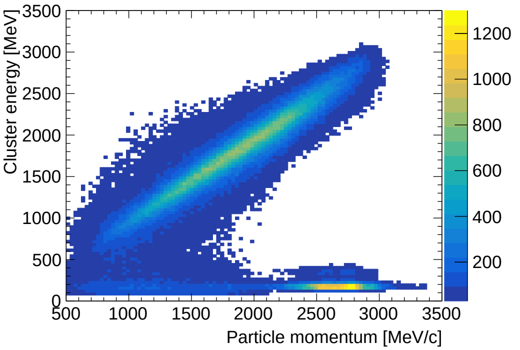

Early to late effects

- unaccounted variations of conditions during muon fill time can induce biases on ω_a fit result

example of early-to-late effect: phase variation due to muon loss

- $N(t) = N_0 e^{-t/\tau_\mu}\,[1 + A\cos(\omega_a t + \varphi)]$ phase $\varphi =$ muon spin-momentum angle at injection
- muon loss depends on momentum $\Rightarrow$ muon sample momentum varies $\bar{p} = \bar{p}(t)$
- single muon phase depends on momentum (because of production chain) $\bar{\varphi} = \bar{\varphi}(\bar{p})$
- at first order $\bar{\varphi}(t) = \bar{\varphi}_0 + \frac{d\bar{\varphi}}{dt} t = \bar{\varphi}_0 + \frac{d\bar{\varphi}}{d\bar{p}}\frac{d\bar{p}}{dt} t \simeq \bar{\varphi}_0 + \bar{\varphi}' t$
- muon rate modulation $\cos(\omega_a t + \bar{\varphi}(t)) \simeq \cos\left(\omega_a t + \bar{\varphi}_0 + \bar{\varphi}' t\right) = \cos[(\omega_a + \bar{\varphi}')t + \bar{\varphi}_0]$
  $\Rightarrow$ fit result for ω_a is biased when muon sample phase varies in the fit time window
- note: muon loss phase effect is different and additional to muon loss effect on positron rate

other early to late effects

- variation of calorimeter gain (corrected before the wiggle plot fit)
- variation of pileup (proportional to $[N(t)]^2$, corrected before the wiggle plot fit)
- variation of beam average position and size (phase acceptance)
- transient magnetic field due to electric quadrupoles plates vibration
- transient magnetic field due to kicker eddy currents

Electric field correction $C_e = +489 \pm 53\,\text{ppb}$

- compute momentum distribution from electrons detected at early times after injection
  - using cosine Fourier transform of rate vs. time
  - measuring change of shape of rectangular bunches (debunching)
- compute radial muon distribution from momentum distribution
- compute electric field contribution to ω_a due to quadrupoles electric field

cosine Fourier vs. debunching method

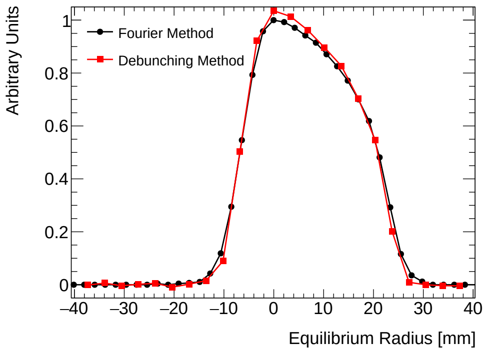

radial distributions in the four datasets

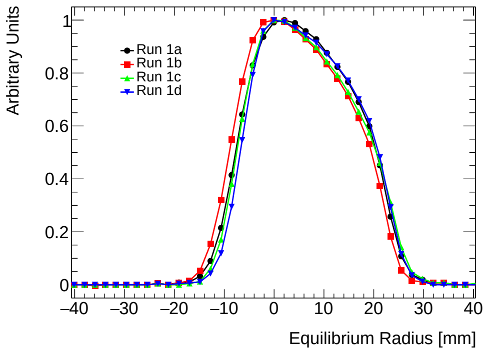

Pitch correction $C_p = +180 \pm 13\,\text{ppb}$

- reconstruct muon vertical position from decay electrons measurend on trackers
- compute corresponding pitch correction to ω_a

vertical decay vertices distribution

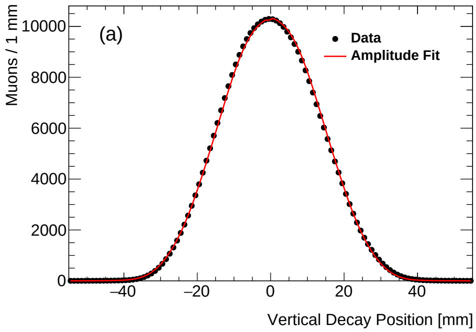

vertical oscittation amplitude distribution

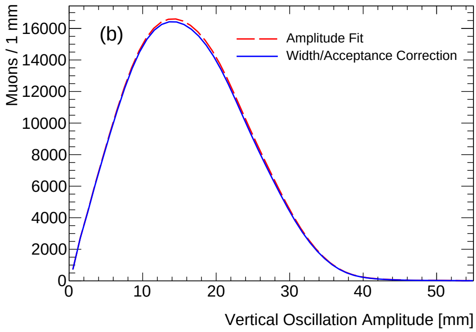

Lost muons phase-variation effect correction $C_{ml} = -11 \pm 5\,\text{ppb}$

measured and simulated $\varphi - p$ correlation

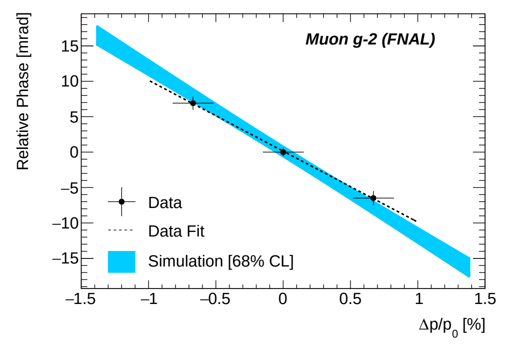

- muon phase depends on momentum
- muon population momentum changes because muon loss probability depends on momentum
- $d\varphi/dp$ measured on dedicated runs by varying magnetic field by -0.68%, +0.68%
- measurement consistent with simulation

estimated $\Delta\varphi(t)$ due to muon loss

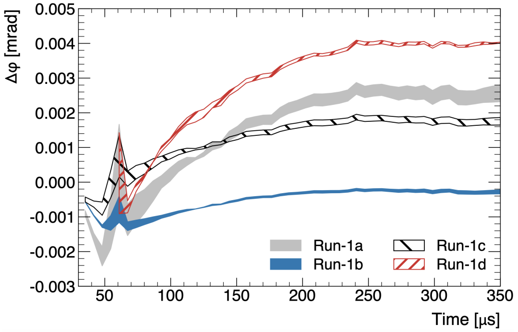

- use delivery ring collimators to change the muon momentum distribution
- muon loss function of time and momentum fitted using simulation-inspired analytic function to model observed beam loss for different muon momentum distributions

Phase-Acceptance correction $C_{pa} = -158 \pm 75$ ppb

- effective phase variation due to variation of beam horizontal and vertical position and spread
- example: $\Delta\omega_a = \frac{d\varphi}{dt} = \frac{d\varphi}{dY_{RMS}} \cdot \frac{dY_{RMS}}{dt}$
- obtained with simulation (← $\frac{d\varphi}{dY_{RMS}}$)
- measured with trackers and extrapolated to whole ring with beam dynamics simulations (← $\frac{dY_{RMS}}{dt}$)

phase as a function of muon position

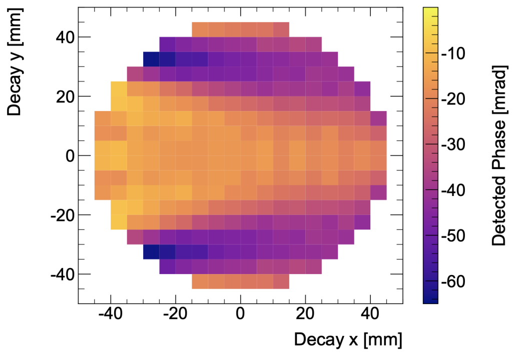

variation of Y_{RMS}

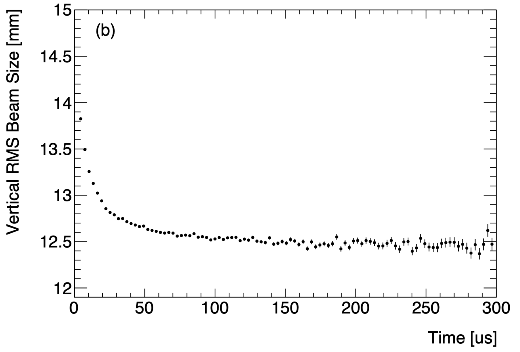

Measuring ω_p / magnetic field with fixed and trolley probes

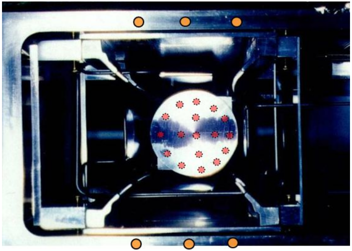

- 378 fixed probes measure continuosly the magnetic field
- 17-probes trolley run along muons path every $\sim$3 days
- fixed probes measurements corrected using trolley measurements

trolley 2D maps

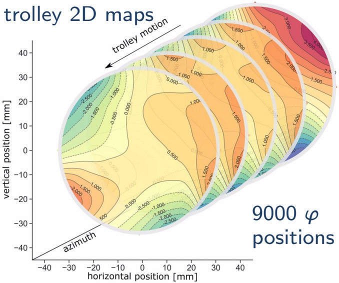

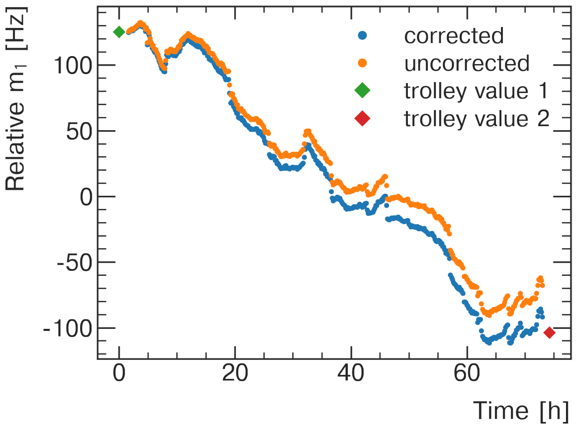

Differential decay corrections

- muon population phase at $t = 0$ depends on muon properties that change during the fill for $t > 0$
  - horizontal displacement and velocity $(x,\ x')$
  - vertical displacement and velocity $(y,\ y')$
  - time of flight from when muon polarization is selected to kicker hit
  - momentum
- injected muons momentum has average and spread at $t = 0$
- momentum average increases for $t > 0$ because slower muons decay earlier on average
- negligible dependence from momentum of vertical displacement and velocity $(y,\ y')$
- other 3 dependences require:
  - differential decay spin-orbit correction
  - differential decay kicker correction
  - differential decay beamline correction

Measuring ω_p magnetic field: calibration of probes

calibration

- each trolley probe calibrated with absolute cylindrical probe placed in the same position inside the storage ring
- absolute cylindrical probe calibrated to reference absolute spherical probe in MRI magnet at Argonne National Laboratory
- absolute spherical probe consistent with novel absolute ^{3}He probe
- 17 probes calibration uncertainty $20 - 48\,\text{ppb}$

reference temperature

- magnetic field measurements corrected to be expressed as $\omega'_p(T)$, precession frequency of shielded proton spin in spherical water sample at reference temperature of 34.7 °C

absolute spherical probe

$\tilde{\omega}'_p(T)$ (magnetic field experienced by the muons) measured to 56 ppb

- tracker reconstructs muons decay vertices in parts of storage region
- beam dynamics simulation used to extrapolate to whole storage region
- magnetic field map averaged over muon distribution
- two independent groups did the measurement, one additional group the calibration